Laser-Induced Nonlinear Dynamics in a Nematic Liquid-Crystal Film

E. Santamato, G. Abbate, P. Maddalena, and L. Marrucci
Dipartimento di Scienze Fisiche, Universita di Napoli, Napoli, Italy

Y. R. Shen
Department of Physics, University of California, Berkeley, California 94720
(Received 27 December 1989)

An elliptically polarized cw laser beam propagating in a nematic liquid-crystal film can induce molecular reorientation and lead the system through various dynamic regimes: torsional oscillations, precession, nutation with precession, and others.

PACS numbers: 61.30.Gd, 42.65.−k, 64.70.Md

Laser-beam propagation in a nematic liquid-crystal (LC) film is a fascinating problem. Not only does it exhibit some very unique, highly nonlinear optical phenomena, but it also displays an unusually rich nonlinear dynamical behavior. It has been demonstrated that a sufficiently strong laser field can induce a Fréedericksz transition (an orientational transition) in a nematic film.[1] Consider a homeotropic film with molecules aligned parallel to the surface normal. Above the transition threshold, a linearly polarized beam normally incident on the film can distort the homeotropic alignment by reorienting the molecules against the elastic torque, while a circularly polarized beam can, in addition to the distortion of alignment, cause the molecules to precess uniformly about the surface normal.[2] The latter is the consequence of a constant rate of deposition of angular momentum from the field to the medium.[2] With an elliptically polarized beam, the situation is even more intriguing as we will now report. The main difference between circular and elliptical input polarizations is that, in the former case, the molecular reorientation first breaks the azimuthal symmetry of the system (field and matter). This yields characteristically different results in the two cases. The elliptically polarized input can lead the system through various dynamic regimes: torsional oscillation, nonuniform precession, nutation superimposed on precession, and others. Experimental observations are in good agreement with theoretical predictions from a continuum model of laser-beam propagation in an anisotropic fluid.

In our experiment, the sample studied was a 75-μm homeotropic film of 4-cyano-4′-pentyl-biphenyl (5CB) sandwiched between two surfactant-coated glass slides. An Ar^+-laser beam, focused to 120 μm and normally incident on the sample, was used to pump the sample. The induced time-dependent molecular reorientation was probed by a counterpropagating He-Ne laser beam focused to 70 μm in the same region. The probe beam was circularly polarized and the output from the sample along the surface normal $\hat{\mathbf{z}}$ was analyzed by a heterodyne polarimeter described elsewhere.[3] This apparatus allowed a real-time monitoring of the output polarization state which is specified by the ellipticity S_3 and the angle ψ between the major axis of the polarization ellipse and a reference axis $\hat{\mathbf{x}}$ in the plane of the film. With the probe beam circularly polarized we can easily show that

$$S_3=\sin\left[(2\pi/\lambda)\int_0^d \Delta n(z)dz\right],$$
$$\Delta n(z)=\frac{n_o n_e}{(n_e^2\cos^2\theta+n_o^2\sin^2\theta)^{1/2}}-n_o, \tag{1}$$

where n_o and n_e are the ordinary and extraordinary refractive indices of the LC medium, respectively, $\theta(z,t)$ is the polar angle of the LC director $\hat{\mathbf{n}}$ at (z,t), λ is the wavelength of the probe beam, and d is the sample thickness.

The data were taken by keeping the polarization of the pump beam fixed and varying the pump intensity in 5-mW steps. Following each intensity change, the system generally went through a transient period (~30–60 sec) and settled into a steady state. We found that the system in steady state can exhibit various dynamic behaviors depending on the ellipticity $S_{3p}\equiv\sin 2\chi$ and the intensity I of the pump beam. The observations are summarized in Fig. 1(a), where the observed steady states for various sets of (I,χ) are marked. To avoid inaccuracy in the determination of absolute intensities, the normalized pump intensity $I/I_{\rm th}^0$ is used in the figure, with $I_{\rm th}^0$ referring to the threshold intensity needed for a linearly polarized pump beam to induce the Fréedericksz transition in the medium.[4]

Figure 1(a) shows that, depending on I and χ, the system can fall into different dynamic regimes. Let us start with an elliptically polarized pump beam with a certain ellipticity S_{3p} (say, $\chi\sim\pi/8$). No molecular reorientation in the sample was observed if I was less than the threshold intensity $I_{\rm th}(\chi)$ for the Fréedericksz transition.[4] Just above the threshold, the output was characterized by equilibrium values (S_3,ψ) with small random fluctuations around it. This indicates that the director $\hat{\mathbf{n}}(z)$ was reoriented to a new equilibrium position but not highly stable. With higher pump intensity, the weak fluctuations became stronger and more regular, and

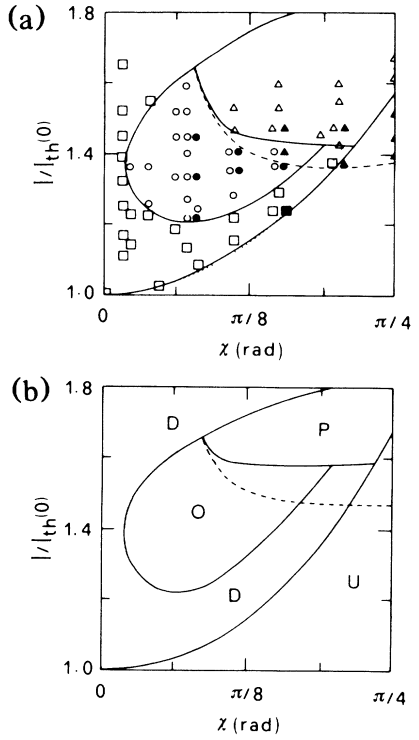

FIG. 1. "Phase" diagrams of various dynamic regimes in the (I,χ) plane. (a) Experimental observations: squares, circles, and triangles denote distorted-equilibrium, persistent-oscillation, and precession-nutation states, respectively. Open symbols refer to states obtained with increasing laser intensity, and solid symbols to states with decreasing intensity. (b) Theoretical simulation. *U*, *D*, *O*, and *P* refer to undistorted, distorted-equilibrium, persistent-oscillation, and precession-nutation regimes, respectively. Solid lines describe boundaries between different dynamic regimes. The dashed line describes the boundary at which *P* switches back to *U*, *D*, or *O* as the pump intensity decreases.

finally appeared as regular persistent oscillations. An example of the persistent oscillation is shown in Fig. 2. This corresponds to a libration of $\hat{\mathbf{n}}$. The transition from the noisy stable state to the persistent oscillation was gradual and smooth. As the pump intensity further increased beyond another critical value I_c, the probe output exhibited a continuous nonuniform rotation of ψ as well as an oscillation in S_3, as illustrated in Fig. 3. This manifests a combined motion of nonuniform precession and nutation of $\hat{\mathbf{n}}$ about the surface normal $\hat{\mathbf{z}}$. The transition to this dynamic regime with increasing I was rather abrupt. With decreasing I, the system returned to the persistent-oscillation regime, but at a lower critical value I_c'. In other words, there was a hysteresis effect in the transition between persistent oscillation and precession and nutation, suggesting that the transition is of first order. As I was further reduced, the system eventually made a sudden transition back to the deformed equilibrium state.

If the ellipticity of the pump polarization was reduced,

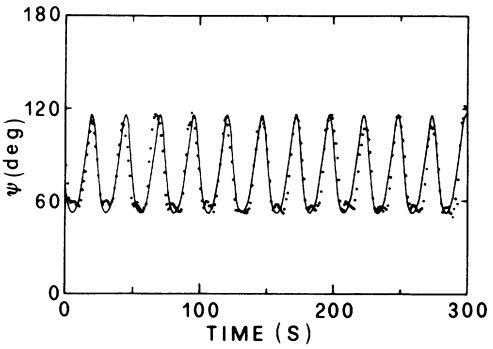

FIG. 2. Persistent oscillation of $\psi(t)$ observed with $\chi=0.35$ rad and $I/I_{th}^{0}=1.4$. The solid line is a theoretical fit.

it was found that with increasing I, the system no longer went into the precession-nutation regime but simply changed from persistent oscillation to a stable equilibrium regime. With further reduction of the pump ellipticity, even the persistent-oscillation regime disappeared. On the other hand, when the elliptical pump polarization became more and more circular, the system would skip the persistent-oscillation regime and switch directly from homeotropic alignment to uniform precession at the Fréedericksz transition threshold. With decreasing I, it

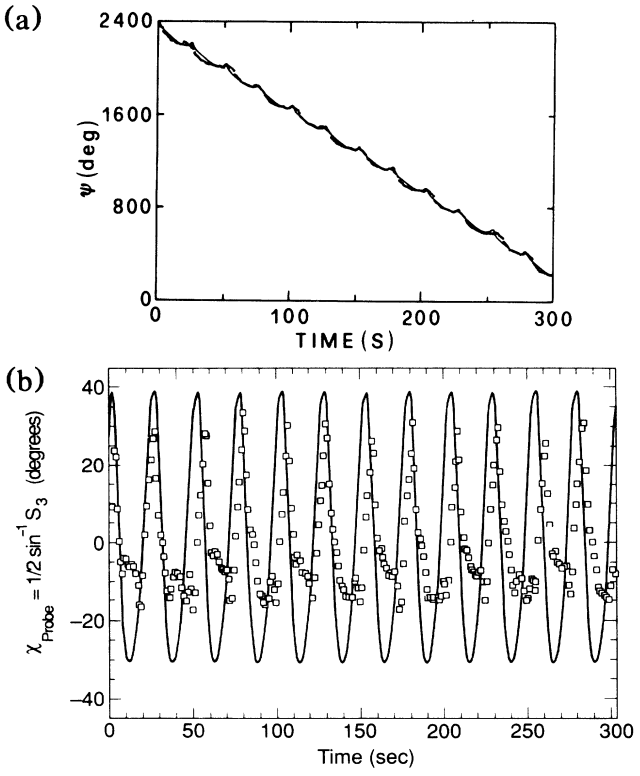

FIG. 3. Precession and nutation of the director as observed by a probe beam. The pump beam was characterized by $\chi=0.5$ rad and $I/I_{th}^{0}=1.5$. (a) ψ vs t exhibiting a nonuniform precession of the director $\hat{\mathbf{n}}$. (b) $\chi_{probe}=\frac{1}{2}\sin^{-1}S_3$ vs t manifesting the nutation of $\hat{\mathbf{n}}$.

switched back to the homeotropic alignment at a lower threshold value. All these features are noted in Fig. 1(a).

Theoretically, the equation of motion governing the director $\hat{\mathbf{n}}$ is the torque-balancing equation

$$\tau_v+\tau_e+\tau_o=0\,, \tag{2}$$

where τ_v, τ_e, and τ_o are viscous, elastic, and optical torques in the medium, respectively. If the backflow effect is neglected, $\tau_v=\gamma(\hat{\mathbf{n}}\times\partial\hat{\mathbf{n}}/\partial t)$ is assumed, with γ being the viscosity coefficient,[5] and the reduced Stokes vector[6] $\mathbf{S}=(S_1,S_2,S_3)$ is used to describe the polarization state of the laser beam in the medium, then Eq. (2) yields[7]

$$\begin{aligned}
&-\gamma\sin^2\theta\frac{\partial\phi}{\partial t}+\frac{\partial}{\partial z}\left[(k_{22}\sin^2\theta+k_{33}\cos^2\theta)\sin^2\theta\frac{\partial\phi}{\partial z}\right]+\frac{I\Delta n(\theta)}{c}(S_2\cos2\phi-S_1\sin2\phi)=0\,,\\
&-\gamma\frac{\partial\theta}{\partial t}+[k_{33}-(k_{33}-k_{11})\sin^2\theta]\frac{\partial^2\theta}{\partial z^2}-(k_{33}-k_{11})\sin\theta\cos\theta\left(\frac{\partial\theta}{\partial z}\right)^2\\
&\qquad-\sin\theta\cos\theta[k_{33}-2(k_{33}-k_{22})\sin^2\theta]\left(\frac{\partial\phi}{\partial z}\right)^2+\left(\frac{I}{2c}\right)\frac{\partial\Delta n}{\partial\theta}(1+S_1\cos2\phi+S_2\sin2\phi)=0\,.
\end{aligned} \tag{3}$$

The variation of the beam polarization in the medium is of course governed by Maxwell equations. In the slowly-varying-amplitude approximation, one can show that the reduced Stokes vector obeys a simple precession equation,[6,8]

$$\partial\mathbf{S}/\partial z=\boldsymbol{\Omega}\times\mathbf{S}\,, \tag{4}$$

with $\boldsymbol{\Omega}=(2\pi/\lambda)(\cos2\phi,\sin2\phi,0)$. Equations (3) and (4) together with the boundary conditions $\theta(0,t)=\theta(d,t)=0$ and $\partial\phi(0,t)/\partial z=\partial\phi(d,t)/\partial z=0$ allow us to find $\theta(z,t)$, $\phi(z,t)$ [and hence $\hat{\mathbf{n}}(z,t)$], and $S(\hat{z},t)$. We note that an integration of the first equation in Eq. (3), with the help of Eq. (4) and the boundary conditions, leads directly to the expression for angular momentum conservation,[3]

$$\gamma\int_0^d\sin^2\theta\frac{\partial\phi}{\partial t}dz=\frac{I}{\omega}[S_3(d)-S_3(0)]\,. \tag{5}$$

If the system is in an equilibrium state, $\partial\phi/\partial t=0$ and we expect $S_3(d)=S_3(0)$. This is indeed what we observed in the experiment.

We have solved Eqs. (3) and (4) with the boundary conditions numerically. The following material constants of 5CB reported in the literature[7,9] were used in the calculation: $k_{11}=0.7\times10^{-6}$ dyn, $k_{22}=0.5\times10^{-6}$ dyn, $k_{33}=0.9\times10^{-6}$ dyn, $n_o=1.52$, and $n_e=1.7$. To simulate the experimental situation, the intensity I was varied in small steps of 5 mW with the input ellipticity fixed. The calculation was able to reproduce semiquantitatively most of the experimental observations. Figure 1(b) depicts the various dynamic regimes of the system predicted by the calculation. Comparison with the experimental result in Fig. 1(a) shows that although the two "phase" diagrams do not match qualitatively in all regimes, all phases observed in the experiment are reproduced by the calculation in proper successive order. Even the observed hysteresis between persistent oscillation and precession and nutation reappears in the calculation. The experimental results in Figs. 2 and 3 can also be fitted fairly well by the same calculation; in addition, $\gamma=35$ cP for Fig. 2 and $\gamma=60$ cP for Fig. 3. The different values of γ may mean different average viscosities in the two different dynamic regimes, but they fall in the range of $\gamma=30$–90 cP reported in the literature for 5CB.[7] We have also measured and calculated the period of the persistent oscillation as a function of I at $\chi=0.35$ and found a semiquantitative agreement between theory and experiment. In particular, the experimental observation of the appearance of minimum period of oscillation as I varies is confirmed by the calculation. This general fair agreement between theory and experiment is remarkable considering the rather crude approximations invoked in the theory.

Physically, it is the interplay between optical-field-induced molecular reorientation and birefringence-effected beam polarization change that leads to the various dynamic behaviors. In contrast to the case of circularly polarized input, the elliptically polarized input defines the major axis of birefringence at $z\sim0$ and produces an optical torque on the molecules that varies along z, sometimes positive and sometimes negative. The calculation shows that just above the transition threshold, $\hat{\mathbf{n}}(z)$ and $\mathbf{S}(z)$ undergo a damped oscillation to reach the new equilibrium state [with $S_3(d)=S_3(0)$]. Damping comes from viscosity. The noise observed in the experiment is presumably due to the system response to the laser fluctuations in this marginally stable regime. With increasing laser intensity, viscous damping becomes less effective and soon $\hat{\mathbf{n}}(z)$ and $\mathbf{S}(z)$ go into persistent oscillation. For $I>I_c$, the optical torque on the molecules along z no longer changes sign, and so is the angular momentum deposited by light into the medium. This sets $\hat{\mathbf{n}}(z)$ into a precession about $\hat{\mathbf{z}}$ in conjunction with a nutation. Our calculation also shows that further increase of the beam intensity can actually decrease the angular momentum $I|S_3(d)-S_3(0)|/\hbar$ deposited into the medium, and when $S_3(d)=S_3(0)$, the system switches back to an equilibrium state. In this state, $\hat{\mathbf{n}}(z)$

is twisted along z and the output polarization is rotated from the input one. Unfortunately, the required laser intensity is generally too high so that we were not able to explore this regime in detail in our experiment.

In summary, we have found, both theoretically and experimentally, that an elliptically polarized input laser beam with intensity above the Fréedericksz transition can induce a successive series of orientational dynamics in a homeotropic liquid-crystal film as reflected in the time-dependent variation of the output beam polarization. These nonlinear dynamical and optical effects are results of the influence of beam polarization and molecular orientation on each other, angular momentum exchange between the two, and balance or imbalance of optical, elastic, and viscous torques in the film.

This work was supported by Ministero della Pubblica Instruzione and by Comitato Nazionale delle Ricerche, Italy. E.S. and Y.R.S. acknowledge NATO Grant No. 0463/87. Y.R.S. was supported by National Science Foundation–Solid State Chemistry Grant No. DMR-8717137. We also wish to thank A. Boiano for his support in setting up the electronic equipment.

[1]See, for example, S. D. Durbin, S. M. Arakelian, and Y. R. Shen, Phys. Rev. Lett. **47**, 1411 (1981).

[2]E. Santamato, B. Daino, M. Romagnoli, M. Settembre, and Y. R. Shen, Phys. Rev. Lett. **57**, 2423 (1986); **61**, 113 (1988).

[3]R. Calvani, R. Caponi, and F. Olsternino, Opt. Commun. **54**, 63 (1985).

[4]The threshold intensity for a pump beam with ellipticity χ is given by $I_{\rm th}(\chi)=2I_{\rm th}^{0}/(1+\cos 2\chi)$; see B. Ya. Zel'dovich and N. V. Tabirian, Zh. Eksp. Teor. Fiz. **82**, 167 (1982) [Sov. Phys. JETP **55**, 99 (1982)].

[5]F. M. Leslie, Quart. J. Mech. Appl. Phys. **19**, 357 (1966). Here, the velocity gradients in the fluid are assumed negligible.

[6]H. Kubo and R. Nagata, J. Opt. Soc. Am. **73**, 1719 (1983).

[7]R. Skarp, S. T. Lagerwall, and B. Stebler, Mol. Cryst. Liq. Cryst. **60**, 215 (1980).

[8]E. Santamato, G. Abbate, and P. Maddalena, Phys. Rev. A **38**, 4323 (1988).

[9]S. Faetti, M. Gatti, and V. Palleschi, Phys. Rev. Appl. **21**, 451 (1986).